

Proceedings of the TensiNet Symposium 2019

Softening the habitats | 3-5 June 2019, Politecnico di Milano, Milan, Italy
Alessandra Zanelli, Carol Monticelli, Marijke Mollaert, Bernd Stimpfle (Eds.)

Inflatable beams subjected to axial forces

Jean-Christophe THOMAS*, Anh LE VAN^a

*GeM (Institute for Research in Civil and Mechanical Engineering),
Université de Nantes-Ecole Centrale Nantes, UMR CNRS 6183
2, rue de la Houssinière, BP 92208, 44322 Nantes Cedex 3, France
jean-christophe.thomas@univ-nantes.fr

^aGeM (Institute for Research in Civil and Mechanical Engineering),
Université de Nantes-Ecole Centrale Nantes, UMR CNRS 6183

Abstract

The inflatable beam is one of the simplest models to understand the mechanics of the inflatable structures in general. In this study, we address the problem of an inflatable beam subjected to compressive and transverse loads. Although the strength of materials for inflatable beams is now well established for inflatable beams subjected to transverse loads, the case of the combined axial and transverse loads has received few studies. Contrary to what one may think, one must not superimpose the two loads in as much as the axial loads modify the stiffness of the beam. For example, a compressive load counteracts the effect of the pressure on the end surface of the beam and reduces its stiffness. The authors present here some new formulations for the bending of inflatable beams subjected to compressive forces.

Also addressed in this work is the buckling of inflatable beams subjected to compressive loads. Analytical formulas are proposed, taking into account the effect of the internal pressure.

Keywords: lightweight structure, structural membrane, pneumatic structure, inflatable beam, buckling

DOI: 10.30448/ts2019.3245.32

Copyright © 2019 by Jean-Christophe Thomas and Anh Le Van. Published by Maggioli SpA with License Creative Commons CC BY-NC-ND 4.0 with permission.

Peer-review under responsibility of the TensiNet Association

1. Introduction

Pneumatic structures are an important part of lightweight structures. They are very various, and some of them can be seen of the website (Tensinet association website). They can be divided into different families: air-supported structures which are mono-membranes, air-inflated structures – also named here inflatables, which are generally composed of air beams or/and air cushions, and hybrid structures, which can be composed of both. Air beams are the simplest model to understand the behavior of inflatable structures: deflection of the beam, apparition of wrinkle, collapse of the beam under bending, buckling. Some previous studies have been conducted on these key-points and allow predicting precisely the behavior of inflatable beams (Fichter 1966, Le Van and Wielgosz 2005, Nguyen and al. 2013, 2015, Thomas and Bloch 2016). Knowing precisely the performance of the models used to design membrane structures is a current and important issue. Working Group 5 of CEN TC 250 is working on rules of design in Europe (Eurocode), which should be obtained from reliability analysis. In this frame, it is of importance to know the performance of the models used to conduct the analysis. The analytical models used to calculate inflatable beams submitted only to transverse loads have been compared with 3D simulation results and with experiments. These models have been used to conduct a reliability analysis of a pedestrian inflatable bridge (Thomas and al. 2018). These studies should now be extended to the case of combined loads.

Some inflatable structures are submitted to combination of loadings, for example bending and compression. This can be the case of an inflatable mast supporting heavy loads due to lighting systems, monitoring systems, etc. It is usual to superimpose the effects of the actions in the case of beams made of conventional materials (steel, aluminum, concrete..). But the stiffness of inflatable beams comes from the pretension due to the internal pressure. The pressure applied on the ends of the beams leads to a normal load, which is transmitted in the membrane along the beam and gives a reserve of axial positive stresses. This study addresses the influence of compressive axial forces that counteract the pretension in the case of a combination compression-bending for an inflatable beam.

To answer this question, we will first present the model of a uncompressed inflatable beam and explain how to adapt logically the results to answer our problem. Then, in a second part, we present a new formulation dedicated to the deflection of inflatable beams under compression. We then give the formulations for the buckling and propose finally a comparison between our analytical results and numerical results obtained with a 3D membrane code.

All the 3D numerical computations of this study are done with a homemade code dedicated to membrane structures. It is based on the total Lagrangian formulation. The non linear equations are solved by an iterative Newton scheme. The material can be isotropic or orthotropic.

2. Behaviour of inflatable beams subjected to transverse loads

For this study, the membrane is supposed orthotropic, and one orthotropy direction is supposed parallel to the axis of the beam. This will represent a coated fabric for which the warp is aligned with the axis of the beam. The local orthotropy basis is $(\vec{e}_\ell, \vec{e}_t, \vec{e}_z)$, where ℓ means axial, and t refers to transverse, Fig. 1.

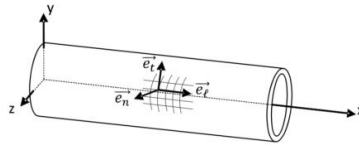


Figure 1: local orthotropy basis

2.1. The different steps

Let us consider an inflatable beam subjected to a transverse load applied in its middle. Figures 2 and 3 present some key-points of its behaviour. Figure 2.a shows the step of inflation. This step is particularly important because it gives the beams its stiffness. The red mesh corresponds to the beam submitted to a very low pressure, which allows balancing the own weight of the fabric and ensuring the section of the beam to be quasi-circular. This corresponds to the natural state of the beam, which is denoted by the sign Φ in the following. For example, R_Φ and L_Φ are the radius and the length of the beam in the natural state. The grey mesh corresponds to the beam at the end of the pressurization. This state is called initial state. R and L are the radius and length in this initial state. Figure 2.b shows the deflected beam. Once loaded transversely, the beam attains the so-called actual state. It has been experimentally verified that the deflection of the beam depends linearly on the load provided that a certain level of loading is not exceeded. Current strength of material theory studies the behaviour between the initial and the actual state. For beams made of more conventional materials (steel, aluminium, concrete, wood...), there is no natural state.

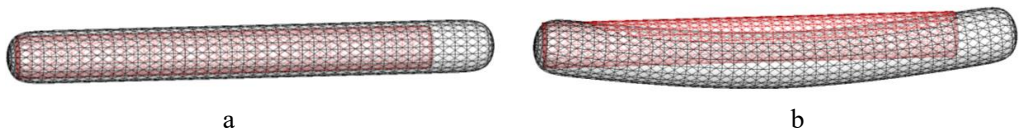


Figure 2: inflation and bending of an inflatable beam

The level of loading mentioned not to be exceeded to remain in the linear domain corresponds to the apparition of plasticity in the cases of conventional materials. The case of inflatable beams is different. The first phase of linear behaviour ends as soon as a wrinkle appears at the upper

surface of the beam in this case. The wrinkling load is reached. Note that the apparition of the wrinkle does not imply the collapse of the beam. There exists a reserve of stiffness. Increasing the load beyond the wrinkling load leads to a propagation of the wrinkle around the section (Fig 3.a) and the collapse occurs when the wrinkle reaches the middle of the beam section (Fig 3.b). This property had been verified theoretically and experimentally verified (Thomas and Bloch 2016).

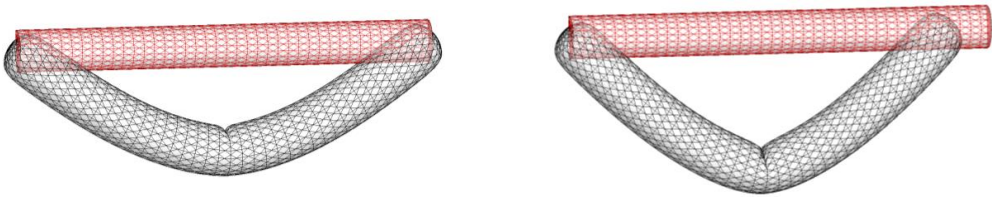


Figure 3: inflatable bended beam- propagation of wrinkle (a) and collapse of the beam (b)

A parallel can be drawn between the plasticity load in the case of conventional materials and the collapse load of inflatable beams.

Not that there exists another specificity of inflatables: when unloaded, they come back to the initial state. It means that, if one neglects the effects of creep, the behaviour is reversible. Reversible collapse is not correct from a semantic standpoint, but it is a physical reality.

2.2. Stresses in the membrane

To understand the behaviour of inflatable beams, it is necessary to detail with precision the distribution of longitudinal stresses in the various cases of loading. Figure 4.a shows the distribution of stresses when no wrinkle appears in the membrane. The longitudinal stresses due to the inflation (in blue) are superimposed with the longitudinal stresses due to the bending (in black), which leads to the final distribution (in blue). Figure 4.b presents the same distribution when a wrinkle appears in the membrane. It happens when a principal stress of the beam vanishes. It allows getting a criterion: the wrinkling load is attained when the longitudinal stress is nil. For example, in the case of a cantilever inflatable beam, one can calculate the wrinkling load function of the pressure p and the geometric parameters:

$$F_W = \frac{p\pi R^3}{2L} \tag{1}$$

Note that the material coefficients (elasticity moduli) do not appear explicitly in the formula. They only impact the length and the radius in the initial state, calculate from the length and the radius in the natural state with the relations:

$$L = L_\phi \left(1 + \frac{pR\phi}{2\phi_{E_\ell}} (2 - \phi_{\nu_{\ell t}}) \right) \quad \text{and} \quad R = R_\phi + \frac{pR_\phi^2}{2\phi_{E_t}} (2 - \phi_{\nu_{\ell t}}) \quad (2)$$

where ϕ_{E_ℓ} and ϕ_{E_t} are the elasticity moduli in the longitudinal and transverse directions, $\phi_{\nu_{\ell t}}$ is a Poisson's coefficient. The shear coefficient is denoted $\phi_{G_{\ell t}}$.



Figure 4: longitudinal stresses in the membrane

2.3. Deflection of the beam

Precise details of the strength of materials theory written at the GeM laboratory can be found in (Le Van and Wielgosz 2005, Nguyen and al. 2013, 2015). We only recall here the key points that will allow to get a linear system of equations useful for the study of an inflatable beam submitted to a combination of axial and transverse loads. The starting point is the total Lagrangian formulation that allows accounting properly the work of the internal pressure. Timoshenko's kinematic must be used for such thin-walled beams to account the effect of shear: the straight section remains in a plane, but doesn't remain orthogonal to the neutral axis of the beam. The constitutive laws of the material are $\Sigma_{xx} = \Sigma_{xx}^0 + E_\ell E_{xx}$ and $\Sigma_{xy} = \Sigma_{xy}^0 + 2G_{\ell t} E_{xy}$, where Σ_{xx}^0 and Σ_{xy}^0 are the stresses in the initial state. It has also been showed that the elasticity moduli used in these constitute laws which refers to the initial state must be calculated from the elasticity moduli of the material in the initial state (Nguyen and al. 2015).

The material coefficients are calculated with two coefficients that characterise the changes of geometry between the natural state and the initial state: $k_x = L/L_\phi$ and $k_\theta = R/R_\phi$.

$$E_\ell = \phi_{E_\ell} \frac{k_x^3}{k_\theta} \quad \text{and} \quad G_{\ell t} = \phi_{G_{\ell t}} k_{\theta x} k_\theta \quad (3)$$

After development of the virtual power principle and a final linearization, the following equations are obtained for a beam subjected to local forces and torques at its extremities .

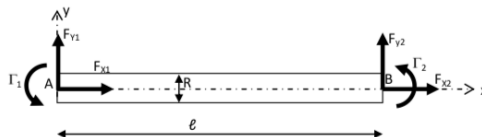


Figure 5: inflatable beam subjected to local forces and torques

$$-\frac{dN}{dx} = 0 \tag{4}$$

$$-(N + kG_{\ell t}S) \frac{d^2v}{dx^2} + (P + kG_{\ell t}S) \frac{d\theta}{dx} = 0 \tag{5}$$

$$\left(E_{\ell}I + \frac{NI}{S}\right) \frac{d^2\theta}{dx^2} + (P + kG_{\ell t}S) \left(\frac{dv}{dx} - \theta\right) = 0 \tag{6}$$

k is a correcting coefficient usually used to account properly the shear in thin membranes. It is equal to 0,5 for circular sections.

The boundary conditions are:

$$N(0) - P = -F_{x1} \quad , \quad N(\ell) - P = F_{x2} \tag{7}$$

$$\begin{aligned} (N + kG_{\ell t}S) \frac{dv}{dx}(0) - (P + kG_{\ell t}S)\theta(0) &= -F_{y1} \\ (N + kG_{\ell t}S) \frac{dv}{dx}(\ell) - (P + kG_{\ell t}S)\theta(\ell) &= F_{y2} \end{aligned} \tag{8}$$

$$\left(E_{\ell}I + \frac{NI}{S}\right) \frac{d\theta}{dx}(0) = -\Gamma_1 \quad \left(E_{\ell}I + \frac{NI}{S}\right) \frac{d\theta}{dx}(\ell) = \Gamma_2 \tag{9}$$

Equations (5) to (8) can be simplified in the case of a beam for which no axial force is superimpose. In this case, equation (4) and (7) show that the normal force N(x) is constant and equal to P. We consider in the following an inflatable cantilever beam only subjected to a load F at its extremity . Equation (5) and (8) lead to

$$(P + kG_{\ell t}S) \left(\frac{dv}{dx} - \theta\right) = F \quad \xrightarrow{\text{yields}} \quad \frac{dv}{dx} = \theta + \frac{F}{P+kG_{\ell t}S} \tag{10}$$

which make evidence of the influence of the shear. Using (6), (9) and $\theta(0) = 0$ gives $\theta(x)$. Equation (10) and the boundary condition $v(0)=0$ lead finally to:

$$v(x) = \frac{F}{E_{\ell}I + \frac{PI}{S}} \left(\ell \frac{x^2}{2} - \frac{x^3}{6}\right) + \frac{Fx}{P+kG_{\ell t}S} \tag{11}$$

Eq. (11) shows the influence of the pressure p on the stiffness. It reinforces the stiffness of the beam, which follow the intuition.

3. Inflatable beams subjected to transverse and compressive loads

The principle of inflatable beams is simple: the effects of the pressure on the two surfaces at each end of the end inducts is equal to P, and is equal to the normal force. An external compression load will then counteract P, and then reduce the stiffness. Let study now the new

problem: a cantilever beam subjected to a transverse load $F_{y2} = F$ and a compression load $F_{x2} = -Q$.

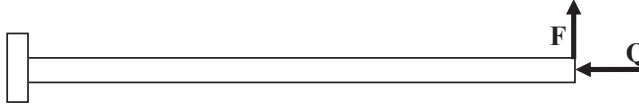


Figure 6: case studied: inflatable beam submitted to a transverse load F and a compressive load Q

3.1. Deflection of the compressed bended beam: adaptation of the uncompressed beam solution

The load Q counteracts the effect off the pressure P on the circular section at the extremity of the beam. It means that the normal force in the beam is no more equal to P, but is equal to $P-Q$. It seems then logical to replace P with $P-Q$ in eq. (11). This leads to the deflection:

$$v(x) = \frac{F}{E_{\rho}I + \frac{(P-Q)I}{S}} \left(\ell \frac{x^2}{2} - \frac{x^3}{6} \right) + \frac{Fx}{(P-Q) + kG_{\ell t}S} \quad (12)$$

This has been done without any demonstration. We propose to solve the problem properly in the following to verify if this solution is valuable or not.

3.2. Deflection of the compressed bended beam: theory

The equations of the theory (4) to (9) are always valuable and allow getting an analytical solution of this new problem. Eqs. (4) and (7) lead to

$$N(x) = P - Q \quad (13)$$

Eqs. (5) and (8) yield to

$$\frac{dv}{dx} - \theta = \frac{Q}{N + kG_{\ell t}S} \theta + \frac{F}{N + kG_{\ell t}S} \quad (14)$$

Including Eq. (13) into (6) allows to eliminate $v(x)$, and gives a second order linear differential equation:

$$\frac{d^2\theta}{dx^2} + \frac{P + kG_{\ell t}S}{N + kG_{\ell t}S} \frac{Q}{E_{\rho}I + \frac{NI}{S}} \theta = - \frac{P + kG_{\ell t}S}{N + kG_{\ell t}S} \frac{F}{E_{\rho}I + \frac{NI}{S}}$$

Introducing the variable $\Omega = \sqrt{\frac{P + kG_{\ell t}S}{N + kG_{\ell t}S} \frac{Q}{E_{\rho}I + \frac{NI}{S}}}$ gives the following equation, for which the solutions are well-known:

$$\frac{d^2\theta}{dx^2} + \Omega^2\theta = - \frac{P + kG_{\ell t}S}{N + kG_{\ell t}S} \frac{F}{E_{\rho}I + \frac{NI}{S}} \quad (15)$$

Finally, the rotation of the section is obtained:

$$\theta(x) = A \cos \Omega x + B \sin \Omega x - \frac{F}{Q}$$

In the case of the cantilever inflatable beam studied here, A and B can be calculated with $\theta(0) = 0$ and eq. (10). This finally gives:

$$\theta(x) = \frac{F}{Q} (\cos \Omega x - 1 + \tan \Omega \ell \sin \Omega x) \tag{16}$$

Knowing that $\frac{dv}{dx} = \frac{P+kG_{\ell t}S}{N+kG_{\ell t}S} \theta + \frac{F}{N+G_{\ell t}S}$ and using the boundary condition $v(0)=0$ gives finally the solution for the deflection:

$$v(x) = \frac{F}{N+kG_{\ell t}S} \left[\frac{P+kG_{\ell t}S}{Q} \left(\frac{\sin \Omega x}{\Omega} - x + \frac{\tan \Omega \ell}{\Omega} (1 - \cos \Omega x) \right) + x \right] \tag{17}$$

This equation could be compared with eq. (11) and eq.(12), but the influence of the compression force Q on the stiffness is not easily understandable in eq. (17) because Ω depends also on Q.

3.3. Deflection of the compressed bended beam for small compressive loads

Let now see what happens if the compression load Q is small. If Q tends to 0, then Ω tends to 0. It is possible to use the Taylor expansion for $\sin \Omega x \approx \Omega x - \frac{\Omega^3 x^3}{6}$, and $\cos \Omega x \approx 1 - \frac{\Omega^2 x^2}{2}$, which finally leads to:

$$v(x) = \frac{F}{N+kG_{\ell t}S} \left[\frac{P+kG_{\ell t}S}{Q} \Omega^2 \left(\ell \frac{x^2}{2} - \frac{x^3}{6} \right) + x \right]$$

Replacing Ω^2 with its value gives:

$$v(x) = F \left[\frac{(P+kG_{\ell t}S)^2}{(N+kG_{\ell t}S)^2} \frac{1}{E_{\ell}I + \frac{NI}{S}} \left(\ell \frac{x^2}{2} - \frac{x^3}{6} \right) + \frac{x}{N+kG_{\ell t}S} \right]$$

The assumption of small compressive loads leads finally to:

$$v(x) = F \left(\frac{1}{E_{\ell}I + \frac{NI}{S}} \left(\ell \frac{x^2}{2} - \frac{x^3}{6} \right) + \frac{x}{N+kG_{\ell t}S} \right) = F \left(\frac{1}{E_{\ell}I + \frac{(P-Q)I}{S}} \left(\ell \frac{x^2}{2} - \frac{x^3}{6} \right) + \frac{x}{(P-Q)+kG_{\ell t}S} \right) \tag{18}$$

One recognizes eq. (12). So, this shows that it is theoretically possible to account the change of the pretension effect due to the compressive loads, by replacing the longitudinal load P do to the pressure inside the beam with P-Q, in the case of small compressive loads. This allows then using the “usual” solution for the deflection with a very little modification.

3.4. Buckling of the beam

When a beam is subjected to a pure compressive load, buckling can occur. This leads to a new limit load F_B that has to be added to the wrinkling load F_w and to the collapse load F_c . To calculate the buckling load, results of paragraph 3.1 have to be used. Eq. (15) gives

$$\frac{d^2\theta}{dx^2} + \Omega^2\theta = 0$$

for which the solution is $\theta(x) = A \cos \Omega x + B \sin \Omega x$. The boundary conditions are $\theta(0) = 0$ (the beam is clamped), and $\frac{d\theta}{dx}(\ell) = 0$ from eq. (10). This leads finally to:

$$\cos \Omega \ell = 0 \xrightarrow{\text{yields}} \Omega \ell = \frac{\pi}{2} + n\pi \quad (n = 1.. \infty)$$

There exist an infinity of solution for Ω . It is then possible to calculate the buckling load:

$$\Omega^2 = \frac{P+kG_{\ell t}S}{N+kG_{\ell t}S} \frac{Q}{E_{\ell}I+\frac{NI}{S}} = \frac{P+kG_{\ell t}S}{P-Q+kG_{\ell t}S} \frac{Q}{E_{\ell}I+\frac{(P-Q)I}{S}}$$

Then:

$$\Omega^2 \left[\frac{Q^2 I}{S} - Q \left(E_{\ell} I + \frac{PI}{S} + \frac{I}{S} (P + kG_{\ell t} S) \right) + (P + kG_{\ell t} S) \left(E_{\ell} I + \frac{PI}{S} \right) \right] = (P + kG_{\ell t} S) Q$$

Finally, if one considers the first term (in bold) to be negligible compared to the others in the preceding equation, it is possible to calculate directly Q . The buckling load of the inflatable beam is then obtained by replacing $\Omega \ell$ with its value $\pi/2$.

$$F_B = \frac{E_{\ell} I + \frac{PI}{S}}{\frac{E_{\ell} I + \frac{PI}{S}}{P+kG_{\ell t}S} + \frac{I}{\pi^2} + \frac{I}{S}} \quad (19)$$

3.5. Wrinkling load for the compressed bended beam

The apparition of wrinkle limits the domain of transverse loads for this study. The wrinkling load for the compressed inflatable beam must be calculated. Fig.7 shows the repartition of the longitudinal stresses due to the loadings. Fig 7.a. corresponds to the repartition of the stresses at the end of the inflation, for which the stresses are well known: $\Sigma_{xx}^0 = pR/2$. The black repartition of stresses in fig.7.b corresponds to the longitudinal stresses due to the compression which are superimposed to the stresses due to the inflation. This leads then to the decrease of Σ_{xx}^0 :

$$\Sigma_{xx}^0 = \frac{P-Q}{2\pi R} = \frac{pR}{2} - \frac{Q}{2\pi R} \quad (20)$$

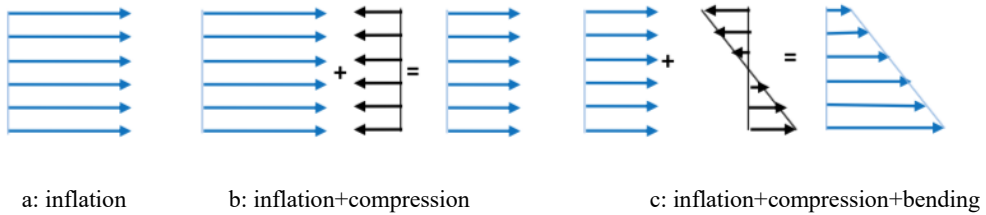


Figure 7: longitudinal stresses in the membrane for an inflatable compressed bended beam

Finally, it is possible to obtain the distribution of stresses for a compressed bended inflatable beam by adding the stresses due to the bending. Considering always the same criterion for the wrinkling load than in paragraph 2.2, this leads finally to:

$$F_W = \frac{p\pi R^3}{2L} - \frac{QR}{2L} \tag{21}$$

4. Analysis of results in a case studied

We present here some results for an inflatable compressed beam. Comparisons are made with the results of the 3D homemade software SAFE dedicated to inflatable structures. For practical reasons, the 3D simulations are conducted on the right configuration of the beam (see fig.8), which is equivalent to the left configuration: clamped compressed inflatable beam.

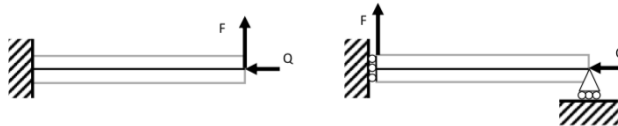


Figure 8: Boundary conditions for a compressed bended beam

The material properties and the geometrical parameters are given table 1.

Table 1: Material coefficients and geometrical parameters for the example

Parameter	Value	
Length in the natural state	L_ϕ	2.5 (m)
Radius in the natural state	R_ϕ	0,125 (m)
Longitudinal elasticity modulus in natural state	${}^\phi E_\ell$	210 (kN/m)
Transverse elasticity modulus in natural state	${}^\phi E_t$	210 (kN/m)
Shear elasticity modulus in natural state	${}^\phi G_{\ell t}$	50 (kN/m)
Poisson's coefficient in the natural state	${}^\phi \nu_{\ell t}$	0,2

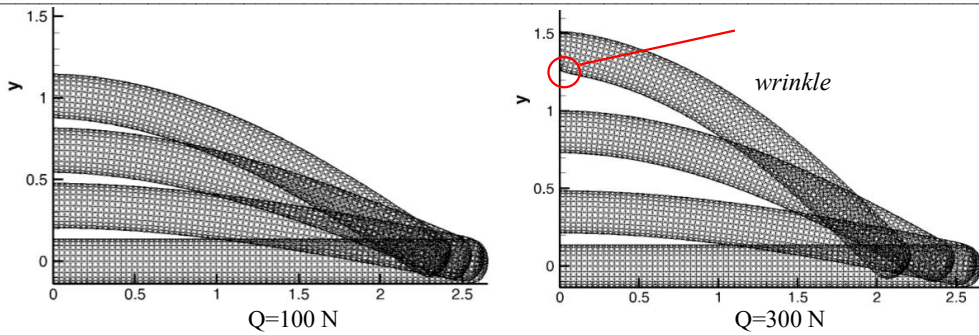


Figure 9: Results of the 3D membrane computations

Figure 9 shows the deflections of the beam for 2 compressive loads. The pressure in both cases is equal to $2 \cdot 10^5$ Pa. Three following increasing transverse loads have been used for each figure: $F=60\text{N}$, 156N and 267N for $Q=100\text{N}$, and $F=61\text{N}$, 169N and 248N for $Q=300\text{N}$. Since the three loads are closed for each series of simulation, the influence of the compressive load is clear. The higher the compressive load, the higher the deflection.

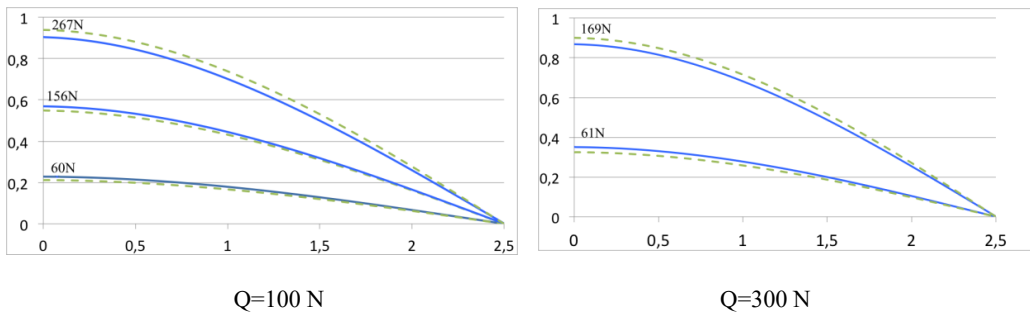


Figure 10: Comparison between the 3D results (blue) and the theoretical results (green)

Figure 10 presents the comparison between the results of the software SAFE and the theoretical results obtained with eq. (17). It shows that the effect of the compressive load is taken into account correctly because the differences between both calculations are less than 7% for the cases studied here. For the case $Q=300\text{N}$, the curves for the highest load are not given because the wrinkle has appeared at the left extremity, as can be seen on figure 9 (right).

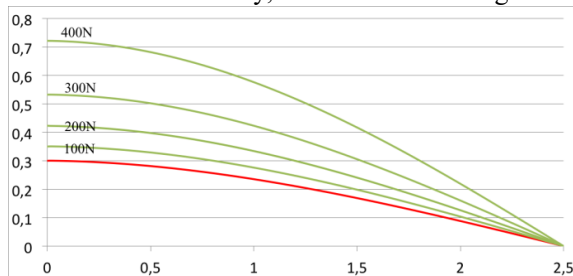


Figure 11: Influence of the compressive load

Fig.11 shows more clearly the effect of the compression. The radius of the beam in its initial state is 0,125m. This means that the force P inside the beam due to the pressure has an order of magnitude of 12kN. The compression loads used here are very small compared to P (less than 4%) here, but has clearly a significant effect. Ignoring the compression lead to an error in the deflection (red curve on fig 11). Moreover, it is also clear that replacing P with $P-Q$ (eq. 12) will not have an effect for the orders of magnitudes that are used in such applications. This formulation is valuable if P and Q are comparable, and for low values of Q .

5. Conclusion

Inflatable beams can be subjected to combination of loads. Although the strength of materials for inflatable beams is now well established for beams subjected only to transverse loads, combinations of loads have not been really investigated. To fill this gap, this study gives analytical solutions for compressed inflatable beams and comparisons with 3D membrane simulations, which have shown the accuracy of the solution. It has also been showed that the beams are very sensitive to the compressive loads.

References

- Tensinet association website. Retrieved from <http://www.tensinet.com>
- Fichter W. (1966), "A theory for inflated thin-wall cylindrical beams", *NASA Technical Note*, NASA TND-3466.
- Le Van A. and Wielgosz C. (2005), "Bending and buckling of inflatable beams: some new theoretical results", *Thin-Walled Structures*, vol 43, pp. 1166-1187.
- Nguyen Q.-T., Thomas J.-C., and Le Van A. (2013), "An analytical solution for an inflated orthotropic membrane tube with an arbitrarily oriented orthotropy basis". *Engineering Structures*, 56 (0), 2013, 1080 - 1091.
- Nguyen Q.-T., Thomas J.-C., and Le Van A. (2015), "Inflation and bending of an orthotropic inflatable beam". *Thin-Walled Structures*, 88 (0), 2015, 129 - 144.
- Thomas J.-C., Bloch A. (2016), "Non linear behaviour of an inflatable beam and limit states", *Procedia Engineering* 155, 2016, 398 – 406
- Thomas J.-C., Schoefs F., Caprani C. & Rocher B. (2018). Reliability of inflatable structures: challenge and first results, *European Journal of Environmental and Civil Engineering*